Induced Li-site vacancies and non-linear optical behavior of doped lithium niobate crystals

D. Xue, K. Betzler *, H. Hesse

Fachbereich Physik, Universität Osnabrück, D-49069 Osnabrück, Germany

Abstract

Second-order non-linear optical (NLO) properties of doped lithium niobate (LN) crystals (abbreviated as M:LN, where $M = Mg^{2+}, Zn^{2+}$, and In^{3+}, respectively) have been quantitatively studied from the chemical bond viewpoint. Our results show that the second-order NLO response of doped LN crystals decreases remarkably with increasing dopant concentration in the crystal. The approximately linear composition-property correlation in these doped LN crystals is quantitatively expressed in the current work. A comparison of the different influences of Mg, Zn and In dopants, respectively, shows that these dopants affect the NLO properties of LN crystals mainly via the number of Li-site vacancies induced. © 2001 Elsevier Science B.V. All rights reserved.

1. Introduction

Due to its large electrooptical and non-linear optical (NLO) coefficients [1,2], lithium niobate, $LiNbO_3$ (LN), is one of the most interesting inorganic NLO materials suitable for numerous applications in optics (holographic storage, electrooptic devices, waveguide structures, solid-state lasers, frequency doublers and mixers, parametric oscillators, etc.). In spite of the massive research on this material in the past decades there are still many open questions concerning e.g., the formation of efficient self-frequency doubled lasers or the suppression of the so-called photorefractive damage.

Usually grown from a congruently melting composition, LN is a typical non-stoichiometric crystal exhibiting a Li deficit of about 1.5%. Thus it contains specific intrinsic defects in its crystal structure – mainly lattice vacancies at Li sites and Nb_{Li} antisite defects [3–6].

A rich variety of rare earth [7,8] and metal ions can be introduced as dopant into the LN lattice, either during the growth process or by post-growth techniques like ion implantation, using He^+ or H^+ [9], or indiffusion, using e.g., Cu [10]. Important photonic applications are thus possible as e.g., holographic memories [11,12], optical demultiplexers [13], or self-frequency doubled lasers [14].

Optical devices fabricated from nominally pure LN usually suffer from so-called optical damage

* Corresponding author. Tel.: +49-541-969-2636; fax: +49-541-969-3512.

E-mail address: klaus.betzler@uni-osnabrueck.de (K. Betzler).

47 due to the photorefractive effect when exposed to
48 intense illumination. This effect can be greatly re-
49 duced by co-doping LN crystals with MgO [15,16],
50 ZnO [17], or In$_2$O$_3$ [18], etc., due to the influence of
51 Mg^{2+}, Zn^{2+}, or In^{3+} on the intrinsic defect struc-
52 ture of LN [18–21]. Yet these defects affect not
53 only the photorefractive but also nearly all other
54 optical properties of LN; their influences on the
55 absorption edge [22] and the refractive indices and
56 the phase matching conditions for different con-
57 figurations of second harmonic generation (SHG)
58 [23–27] have already been studied in some detail.
59   The purpose of the present work is a compari-
60 son of these impurity influences on the NLO re-
61 sponse, i.e., the SHG susceptibility tensor, of LN.
62 As shown previously [28], also the non-linear
63 properties of crystals depend sensitively on the
64 impurity content. Applying the chemical bond
65 viewpoint [29–31], the influence of the dopants on
66 the dielectric response is quantitatively analyzed.

67 **2. Structural analysis of doped lithium niobate**

68   In pure LN of stoichiometric composition, the
69 ideal cation stacking sequence along the polar *c*-
70 axis of the crystal can be described by
71 $\cdots$–Li–Nb–□–Li–Nb–□–$\cdots$, where □ represents
72 for a structural vacancy (an empty oxygen octa-
73 hedron) [3]. This crystal structure is illustrated by
74 Fig. 1. The structural situation changes when do-
75 pants are introduced into the crystal. Nearly all
76 two- or three-valenced dopants are found to oc-
77 cupy Li sites [32,33] – at least at low doping levels
78 (up to some percent). Charge compensation is ac-
79 complished by the formation of an appropriate
80 number of Li vacancies. This modifies the local
81 chemical bonding state in the crystal in a random
82 way, especially for the oxygen atoms around the
83 dopants and the vacancies. As an exact numerical
84 treatment of such a disturbed crystal is not possi-
85 ble to date, one has to introduce some practical
86 simplifications.
87   The chemical bond method [29–31] treats a
88 compound as an infinite network of constituent
89 atoms linked by chemical bonds. For pure crystals,
90 this can be reduced to a finite network comprising
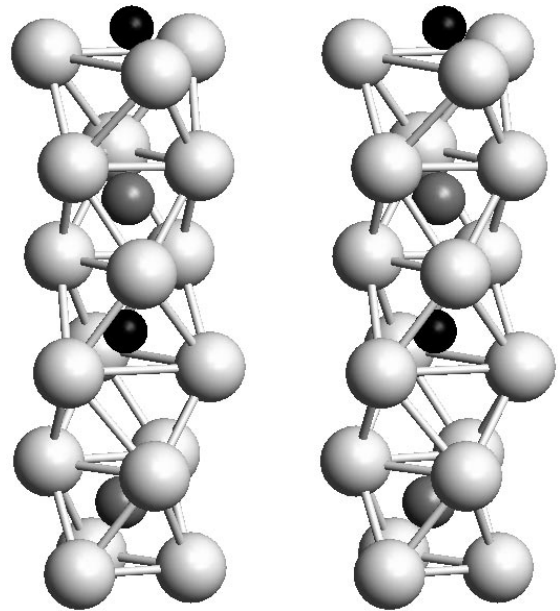91 a single formula unit such as the network of

Fig. 1. Stereoscopic view (to be viewed with crossed eyes) of the ideal crystal stacking sequence of lithium niobate along the crystallographic *c*-axis (light gray: oxygen, dark gray: niobium, black: lithium).

LiNbO$_3$, in which Li$^+$ and Nb^{5+} are six-coordi-   92
nated (with O^{2-} anions) and O^{2-} is four-coordi-   93
nated (with two Li$^+$ cations and two Nb^{5+} 94
cations). The detailed chemical bonding descrip-   95
tion for pure LiNbO$_3$ is shown in Fig. 2(a). In the   96
graphs of Fig. 2, each line represents a different   97
bond, and each atom A in the corresponding lat-   98
tice is assigned a formal charge equal to its atomic   99
valence or oxidation state (V_A) and each bond   100
between atoms A and B is assigned a bond valence   101
(s_{AB}). The sum of the bond valences (each with   102
appropriate algebraic sign according to the bond   103
direction) at each node atom in the network equals   104
its formal charge, the sum around any loop is zero   105
[30,31]   106

$$\sum_B s_{AB} = V_A \quad \text{and} \quad \sum_{loop} s_{AB} = 0. \qquad (1)$$

Calculations of the crystal susceptibility are based   108
on such a suitable decomposition of the crystal   109
into single bonds.   110
    The exact treatment of doped LN would require   111
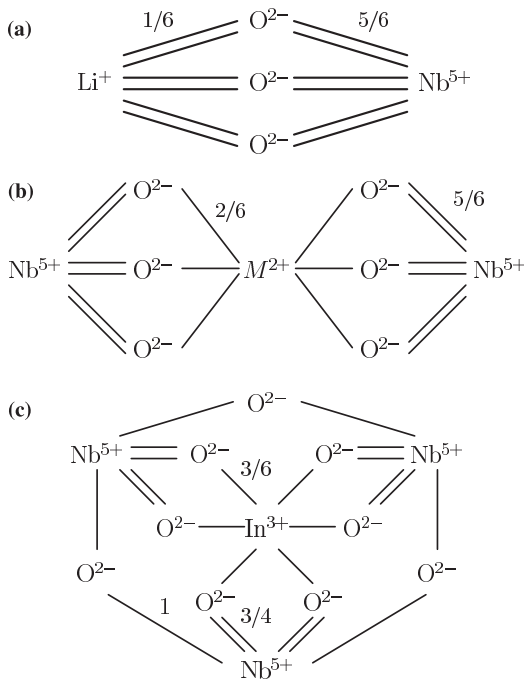a large number of such bond graphs, each de-   112

(a)

Fig. 2. The bond graph of: (a) pure LiNbO₃; (b) M²⁺:LiNbO₃, where M is Mg and Zn, respectively; (c) In³⁺:LiNbO₃. The valences of the atoms and the theoretical valences of the bonds are shown.

113 scribing one of the possible environments around a
114 dopant ion. To avoid such complications with
115 randomly distributed modified bonding situations,
116 we treat doped LN instead as an appropriate
117 mixture of pure LN with pure 'metal' niobate
118 (metal = Mg, Zn, In,...). Of course this approxi-
119 mative approach can not be used in general, albeit
120 it can be successfully applied for the calculation of
121 optical properties. This is due to the fact that op-
122 tical wavelengths are rather large compared to
123 typical interatomic distances, a summation over a
124 fixed distribution of small regions will yield the
125 same optical susceptibility as a summation over a
126 random distribution. Consequently, for the de-
127 scription and decomposition of doped LN, we use
128 the bond graphs of the metal niobates MNb_2O_6
129 (M = Mg, Zn) and $InNb_3O_9$, as shown in Fig.
130 2(b) and (c), in addition to that of pure LN (Fig.
131 2(a)). Thus crystals of doped LN $Li_{1-x}M_{x/2}NbO_3$
132 and $Li_{1-x}In_{x/3}NbO_3$ are formally treated as $(1-x)$
133 $\cdot LiNbO_3 + x/2 \cdot MNb_2O_6$ and $(1-x) \cdot LiNbO_3 +$

134 $x/3 \cdot InNb_3O_9$, respectively. As a further approxi-
135 mation in the calculations, the geometrical struc-
136 ture data for the metal niobates are adopted from
137 pure LN. Generally it must be assumed that the
138 crystal lattice would relax its geometry slightly
139 around dopants and vacancies due to the altered
140 ionic charges. Yet, to date no experimental struc-
141 tural data are available which describe the *relaxed*
142 lattice around impurities in LN correctly.

3. Theoretical method 143

144 As shown in previous works [29] – developed
145 from the dielectric theory of solids [34–36] – the
146 chemical bond method regards certain macro-
147 scopic physical properties of a crystal as a com-
148 bination of the contributions of all constituent
149 chemical bonds. Accordingly, the linear and sec-
150 ond-order NLO properties of a crystal can be
151 calculated using the appropriate geometric sum of
152 the respective properties of its corresponding
153 constituent chemical bonds. On the basis of the
154 crystallographic structure of an assigned crystal,
155 its linear and second-order NLO susceptibilities χ
156 and d_{ij} thus can be written as

$$\chi = \sum_\mu F^\mu \chi^\mu = \sum_\mu N_b^\mu \chi_b^\mu \qquad (2)$$

and 158

$$d_{ij} = \sum_\mu \left\{ \frac{G_{ij}^\mu N_b^\mu (0.5)\{[(Z_A^\mu)^* + n(Z_B^\mu)^*]/[(Z_A^\mu)^* - n(Z_B^\mu)^*]\}f_i^\mu(\chi_b^\mu)^2}{d^\mu q^\mu} \right.$$
$$\left. + \frac{G_{ij}^\mu N_b^\mu s(2s-1)[r_0^\mu/(r_0^\mu - r_c^\mu)]^2 f_c^\mu(\chi_b^\mu)^2 \rho^\mu}{d^\mu q^\mu} \right\},$$
$$(3)$$

160 respectively. Parameters used in Eqs. (2) and (3)
161 include:

F^μ	Fraction of bonds of type μ composing the crystal.
χ^μ	Linear susceptibility contribution from μ type bonds.
N_b^μ	Number of bonds of type μ per cm³.
χ_b^μ	Susceptibility of a single bond of type μ.

G_{ij}^{μ}	Geometrical contribution of chemical bonds of type μ.
$(Z_A^{\mu})^*, (Z_B^{\mu})^*$	Effective number of valence electrons of A and B ions, respectively.
n	Ratio of numbers of two elements B and A in the bond valence equation [37].
f_i^{μ}, f_c^{μ}	Fractions of ionic and covalent characteristics of the individual bonds, $f_i^{\mu} = (C^{\mu})^2 / [(E_h^{\mu})^2 + (C^{\mu})^2]$ and $f_c^{\mu} = 1 - f_i^{\mu}$, where C^{μ}, E_h^{μ} are the average energy gaps due to ionic and covalent effects.
d^{μ}	Bond length of the μ type bonds in Å.
q^{μ}	Bond charge of the μth bond.
s	Exponent in the bond force constant.
$r_c^{\mu} = 0.35 r_0^{\mu}$	Core radius, where $r_0^{\mu} = d^{\mu}/2$ and d^{μ} is the bond length.
$\rho^{\mu} = (r_A^{\mu} - r_B^{\mu}) / (r_A^{\mu} + r_B^{\mu})$	Difference in the atomic sizes, where r_A^{μ} and r_B^{μ} are the covalent radii of atoms A and B, taken from the periodic table of elements.

According to Levine's model [36] the susceptibility χ^{μ} of any bond of type μ is expressed as

$$\chi^{\mu} = (4\pi)^{-1} \left(\hbar \Omega_p^{\mu} \right)^2 \Big/ \left[(E_h^{\mu})^2 + (C^{\mu})^2 \right], \tag{4}$$

where Ω_p^{μ} is the plasma frequency. The average covalent energy gap E_h^{μ} of a bond is given by [34,38]

$$E_h^{\mu} = 39.74 / (d^{\mu})^s, \quad s = 2.48 \tag{5}$$

the average ionic gap C^{μ} by

$$C^{\mu} = b^{\mu} \exp(-k_s^{\mu} r_0^{\mu}) [(Z_A^{\mu})^* - n Z_B^{\mu})^*] / r_0^{\mu}, \tag{6}$$

where $\exp(-k_s^{\mu} r_0^{\mu})$ is the Thomas–Fermi screening factor and b^{μ} is a correction factor of order unity

[38] taking into account the more complex true screening behavior in crystals.

The bond charge q^{μ} can be expressed as [29,37]

$$q^{\mu} = (n_e^{\mu})^* \left[1/(\chi^{\mu} + 1) + f_c^{\mu} (2^{F_c} - 1.1)/N_{\text{cation}} \right] e, \tag{7}$$

where $(n_e^{\mu})^*$ is the number of valence electrons per bond μ, $F_c = \sum_{\mu} N_b^{\mu} f_c^{\mu}$ the crystal covalency, and N_{cation} the cation coordination number.

The geometrical factors G_{ij}^{μ} for the contributions of the respective bond types μ to the tensor coefficients d_{ij} are deduced from the crystal geometry

$$G_{ij}^{\mu} = G_{ikl}^{\mu} = 1/n_b^{\mu} \sum_{\lambda} \alpha_{i,\lambda}^{\mu} \alpha_{k,\lambda}^{\mu} \alpha_{l,\lambda}^{\mu}. \tag{8}$$

The sum on λ is to be taken over all n_b^{μ} symmetry-equivalent bonds of type μ in the unit cell. $\alpha_{i,\lambda}^{\mu}$ denotes the direction cosine of the λth bond of type μ in the unit cell with respect to the ith axis of the optical indicatrix, ij is the contracted form of the full set of indices ikl used in the third rank nonlinear susceptibility tensor.

4. Results and discussion

On the basis of the detailed crystallographic data of pure LN [39] and the modifications for doped LN discussed above, the linear and NLO susceptibilities of all different constituent bonds Li–O, Nb–O, and M–O contained in doped LN are calculated. To increase accuracy, the calculated values of the linear optical susceptibilities were referenced against experimental values. The experimental values of the (ordinary) refractive indices n_o at 1079 nm were taken from previous studies [23,24,26,27] which yield an approximately linear dependence on the dopant concentration at low doping levels:

$$\text{Mg : LN}, \quad n_o = 2.2311 - 0.00085\, c_{\text{Mg}}, \quad c_{\text{Mg}} < 9\%, \tag{9}$$

$$\text{Zn : LN}, \quad n_o = 2.2311 + 0.00079\, c_{\text{Zn}}, \quad c_{\text{Zn}} < 9\%, \tag{10}$$

$$\text{In : LN}, \quad n_\text{o} = 2.2311 - 0.00280\,c_\text{In},$$
$$c_\text{In} < 3\%. \tag{11}$$

210 c denotes the molar percentage of the respective
211 oxide in LN.
212 These experimental references were used to ob-
213 tain the exact correction factors b in Eq. (6).
214 The calculations of the non-linear susceptibili-
215 ties also yield approximately linear dependencies
216 on the dopant concentration, which can be sum-
217 marized by Eqs. (12)–(14):

$$d_{22} = 2.71 \cdot (1 - 0.026\,c_\text{Mg} - 0.023\,c_\text{Zn} - 0.064\,c_\text{In}), \tag{12}$$

219

$$d_{31} = -4.12$$
$$\cdot (1 - 0.028\,c_\text{Mg} - 0.026\,c_\text{Zn} - 0.097\,c_\text{In}), \tag{13}$$

221

$$d_{33} = -22.9$$
$$\cdot (1 - 0.027\,c_\text{Mg} - 0.024\,c_\text{Zn} - 0.082\,c_\text{In}), \tag{14}$$

223 where ds are in pm/V and cs are the molar per-
224 centages of the respective oxides (MgO, ZnO,
225 In_2O_3).
226 For pure LN (i.e., $c_\text{Mg} = c_\text{Zn} = c_\text{In} = 0$) the cal-
227 culated results agree well with experimental data at
228 1064 nm [40]: $d_{22} = 2.1$ pm/V, $d_{31} = -4.3$ pm/V,
229 and $d_{33} = -27$ pm/V, as well as with our previ-
230 ously calculated results at 1064 nm [37].
231 The dependencies of the three tensor coefficients
232 on the doping concentrations show that all coef-
233 ficients decrease approximately linearly with in-
234 creasing doping concentrations. This indicates that
235 the dopants directly or indirectly reduce the
236 acentricity of the material. The decrease is most
237 expressed in In-doped LN, considerably less in the
238 case of Zn or Mg doping, the ratio of the slopes is
239 approximately 4. One explanation for the large
240 difference between three- and two-valent dopants
241 is the scaling used. The d values in Eqs. (12)–(14)
242 are calculated as a function of the 'molar' impurity
243 concentration which usually is referred to the basic
244 oxides composing the material. These basic oxides

245 are Li_2O, Nb_2O_5, MgO, ZnO, and In_2O_3, respec-
246 tively. Taking this and the respective valence state
247 into account, In_2O_3 introduces four times as much
248 Li vacancies as MgO or ZnO into the crystallo-
249 graphic frame of LN. The correspondence between
250 this factor four and the slope ratio discussed above
251 suggests that the reduction in the acentricity of
252 LN, introduced by dopants, is mainly due to the
253 number of Li vacancies, fairly independent of the
254 specific impurity used. A similar factor of 4 is also
255 found when regarding the so-called 'threshold'
256 values [41] for different dopants in LN which were
257 found to be about 6% in the case of Mg and Zn
258 and about 1.5% in the case of In [21]. The fact that
259 the number of Li vacancies strongly affects the
260 NLO properties of LN assures our previous result
261 that the Li places in the crystallographic frame of
262 LN are the sensitive lattice sites, on which dopants
263 (or vacancies) can modify the dielectric properties
264 most effectively [29,37]. Yet this seems to be
265 mainly true for the non-linear properties (i.e., the
266 acentricity) as the linear dielectric properties be-
267 have in a slightly different way: n_o decreases with
268 Mg doping [23], increases with Zn doping [24], and
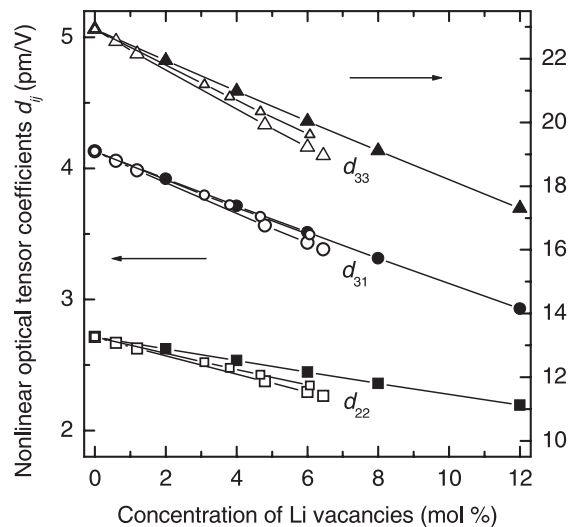269 decreases with In doping [26].

Fig. 3. Non-linear optical tensor coefficients d_{ij} in doped lithi-
um niobate as a function of the lithium vacancy concentration
induced by different dopants. Filled markers: In-doped, small
open markers: Zn-doped, large open markers: Mg-doped lithi-
um niobate.

A plot of the SHG tensor coefficients as a function of the lithium vacancy concentration (Fig. 3) shows the approximately coinciding behavior for all three sorts of dopants discussed here. The behavior of the d values can be described by the global formula

$$d_{ij} = d_{ij}^{\text{pure}} \cdot (1 - 0.023 \cdot c_{\text{VLi}}) \tag{15}$$

with an accuracy of about $\pm 5\%$ for lithium vacancy concentrations c_{VLi} less than 10%. For d_{ij}^{pure} the values given in Eqs. (12)–(14) or the respective experimental values have to be inserted.

5. Conclusion

Dielectric properties of doped LN single crystals at 1079 nm have been quantitatively studied from the chemical bond viewpoint of crystal materials. It is found that different dopants on Li sites in LN affect the second-order NLO response of LN crystals in a different way. Yet all doping dependencies for the dopants regarded here can be described by a global unitary factor when referred to the concentration of lithium vacancies induced by the impurities.

Acknowledgements

References

[1] A. Räuber, Curr. Top. Mater. Sci. 1 (1978) 481.
[2] E. Krätzig, O.F. Schirmer, in: P. Günter, J.P. Huignard (Eds.), Photorefractive Materials and Their Applications, Springer, Berlin, Heidelberg, 1988.
[3] S.C. Abrahams, P. Marsh, Acta Cryst. B 42 (1986) 61.
[4] N. Iyi, K. Kitamura, F. Izumi, J.K. Yamamoto, T. Hayashi, H. Asano, S. Kimura, J. Solid State Chem. 101 (1992) 340.
[5] G. Malovichko, V. Grachev, O. Schirmer, Appl. Phys. B 68 (1999) 785.
[6] F.P. Safaryan, R.S. Feigelson, A.M. Petrosyan, J. Appl. Phys. 85 (1999) 8079.
[7] L.F. Johnson, A.A. Ballman, J. Appl. Phys. 40 (1969) 297.
[8] A. Lorenzo, H. Jaffrezic, B. Roux, G. Boulon, J. Garcia-Sole, Appl. Phys. Lett. 67 (1995) 3735.
[9] J. Rams, J. Olivares, P.J. Chandler, P.D. Townsend, J. Appl. Phys. 87 (2000) 3199.
[10] K. Peithmann, J. Hukriede, K. Buse, E. Krätzig, Phys. Rev. B 61 (2000) 4615.
[11] D. Psaltis, F. Mok, Sci. Am. 273 (1995) 52.
[12] R.M. Shelby, J.A. Hoffnagle, G.W. Burr, C.M. Jefferson, M.-P. Bernal, H. Coufal, R.K. Grygier, H. Guenther, R.M. Macfarlane, G.T. Sincerbox, Opt. Lett. 22 (1997) 1509.
[13] S. Breer, K. Buse, Appl. Phys. B 66 (1998) 339.
[14] E. Montoya, J.A. Sanz-García, J. Capmany, L.E. Bausá, A. Diening, T. Kellner, G. Huber, J. Appl. Phys. 87 (2000) 4056.
[15] G. Zhong, J. Jin, Z. Wu, in: Proceedings of the 11th International Quantum Electronics, Institute of Electrical and Electronics Engineers, New York, 1980, pp. 631–633.
[16] K. Niwa, Y. Furukawa, S. Takekawa, K. Kitamura, J. Cryst. Growth 208 (2000) 493.
[17] T.R. Volk, V.I. Pryalkin, N.M. Rubinina, Opt. Lett. 15 (1990) 996.
[18] T.R. Volk, N.M. Rubinina, Ferroelectr. Lett 14 (1992) 37.
[19] T. Volk, M. Wöhlecke, N. Rubinina, A. Reichert, N. Razumovski, Ferroelectrics 183 (1996) 291.
[20] T. Volk, M. Wöhlecke, N. Rubinina, N.V. Razumovski, F. Jermann, C. Fischer, R. Böwer, Appl. Phys. A 60 (1995) 217.
[21] T.R. Volk, M. Wöhlecke, Ferroelectr. Rev. 1 (1998) 195.
[22] J.J. Xu, G.Y. Zhang, F.F. Li, X.Z. Zhang, Q.A. Sun, S.M. Liu, F. Song, Y.F. Kong, X.J. Chen, H.J. Qiao, J.H. Yao, L.J. Zhao, Opt. Lett. 25 (2000) 129.
[23] U. Schlarb, K. Betzler, Phys. Rev. B 50 (1994) 751.
[24] U. Schlarb, M. Wöhlecke, B. Gather, A. Reichert, K. Betzler, T. Volk, N. Rubinina, Opt. Mater. 4 (1995) 791.
[25] U. Schlarb, A. Reichert, K. Betzler, M. Wöhlecke, B. Gather, T. Volk, N. Rubinina, Radiat. Eff. Def. Solids 136 (1995) 1029.
[26] K. Kasemir, K. Betzler, B. Matzas, B. Tiegel, M. Wöhlecke, N. Rubinina, T. Volk, Phys. Stat. Sol. (a) 166 (1998) R7.
[27] K. Kasemir, K. Betzler, B. Matzas, B. Tiegel, T. Wahlbrink, M. Wöhlecke, B. Gather, N. Rubinina, T. Volk, J. Appl. Phys. 84 (1998) 5191.
[28] D. Xue, K. Betzler, H. Hesse, D. Lammers, Phys. Stat. Sol. (b) 216 (1999) R7.
[29] D. Xue, S. Zhang, Physica B 262 (1999) 78.
[30] I.D. Brown, Acta Cryst. B 48 (1992) 553.
[31] V.S. Urusov, I.P. Orlov, Crystallogr. Rep. 44 (1999) 686.
[32] Y. Ohkubo, Y. Murakami, T. Saito, A. Yokoyama, S. Uehara, S. Shibata, Y. Kawase, Phys. Rev. B 60 (1999) 11963.

365 [33] Y. Furukawa, K. Kitamura, S. Takekawa, K. Niwa, Y.
366   Yajima, N. Iyi, I. Mnushkina, P. Guggenheim, J.M.
367   Martin, J. Cryst. Growth 211 (2000) 230.
368 [34] J.A. Van Vechten, Phys. Rev. 182 (1969) 891.
369 [35] J.C. Phillips, Rev. Mod. Phys. 42 (1970) 317.
370 [36] B.F. Levine, Phys. Rev. B 7 (1973) 2600.
371 [37] D. Xue, S. Zhang, J. Phys.: Condens. Matter 9 (1997) 7515.

[38] B.F. Levine, Phys. Rev. B 7 (1973) 2591.   372
[39] R. Hsu, E.N. Maslen, D. du Boulay, N. Ishizawa, Acta   373
     Cryst. B 53 (1997) 420.   374
[40] D.A. Roberts, IEEE J. Quantum Electron. QE-28 (1992)   375
     2057.   376
[41] K.L. Sweeney, L.E. Halliburton, D.A. Bryan, R. Rice, R.   377
     Gerson, H.E. Tomaschke, J. Appl. Phys. 57 (1985) 1036.   378